Winter 1-8-2013

Ion Transport across Grain Boundaries in Fast Lithium Ion Conducting Glass Ceramics

Bernhard Roling
University of Marburg

Katharina I. Gries
University of Marburg

Michael Gellert
University of Marburg

Kerstin Volz
University of Marburg

Fabio Rosciano
Advanced Technology Division, Toyota Motor Europe, Belgium

See next page for additional authors

Authors
Bernhard Roling, Katharina I. Gries, Michael Gellert, Kerstin Volz, Fabio Rosciano, and Chihiro Yada

Ion Transport across Grain Boundaries in Fast Lithium Ion Conducting Glass Ceramics

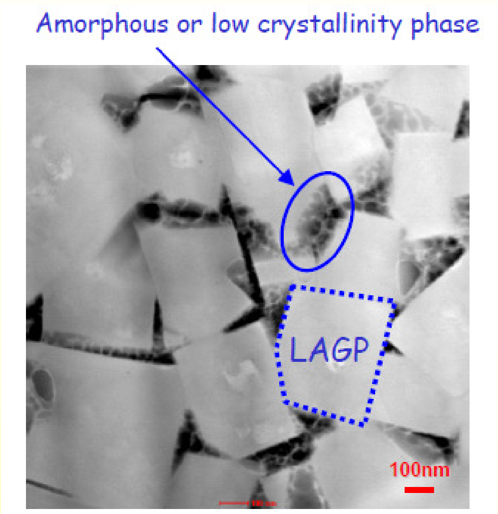

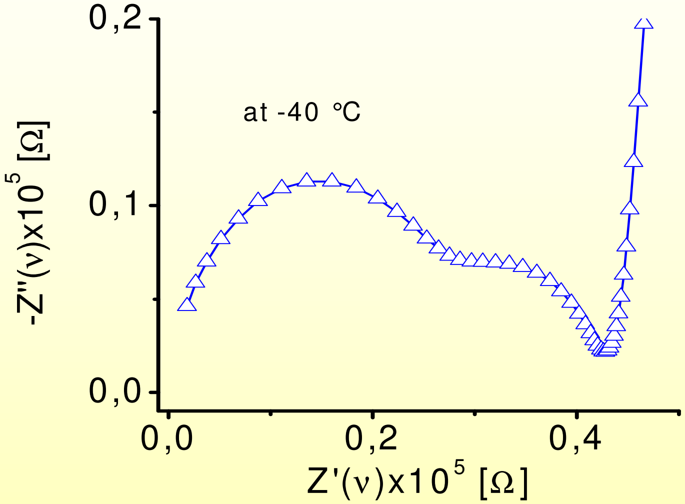

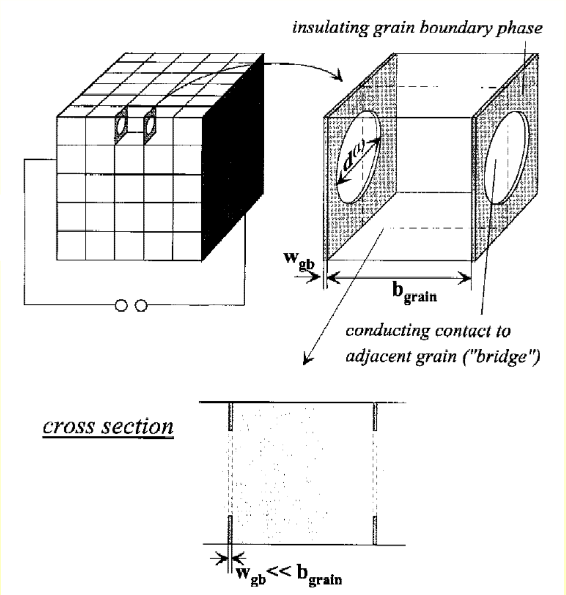

<u>Bernhard Roling</u>, Michael Gellert

Department of Chemistry, University of Marburg

Katharina I. Gries, Kerstin Volz

Department of Physics, University of Marburg

Fabio Rosciano, Chihiro Yada

Advanced Technology Division, Toyota Motor Europe, Belgium

Solid-State Batteries

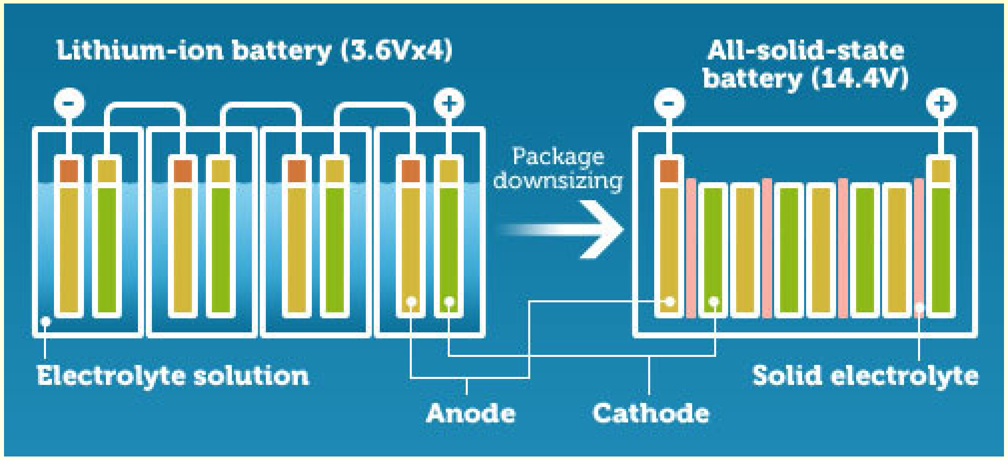

No separation of individual cells

→ More compact packaging

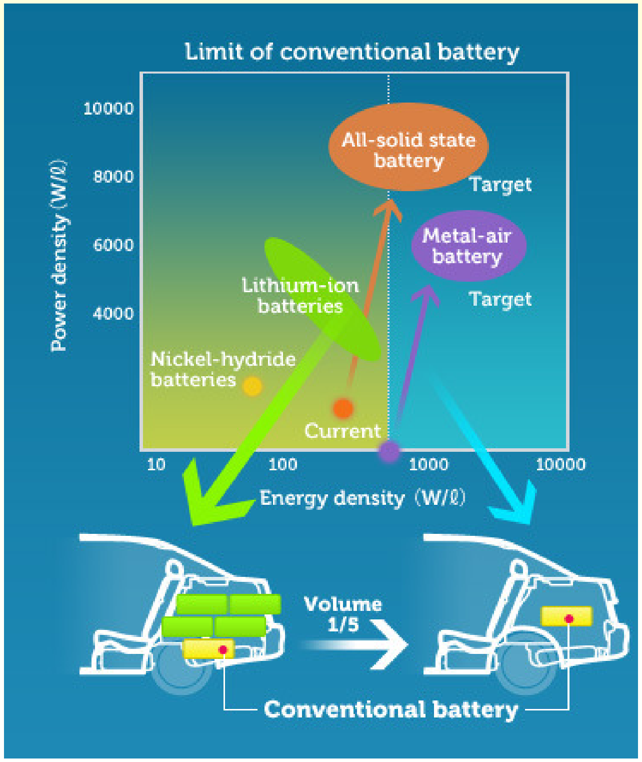

http://www.toyota-global.com/innovation/environmental_technology/next_generation_secondary_batteries.html

Solid-State Batteries

Room-temperature ionic conductivity

$\sigma \approx 10^{-3}$ S / cm

SEI

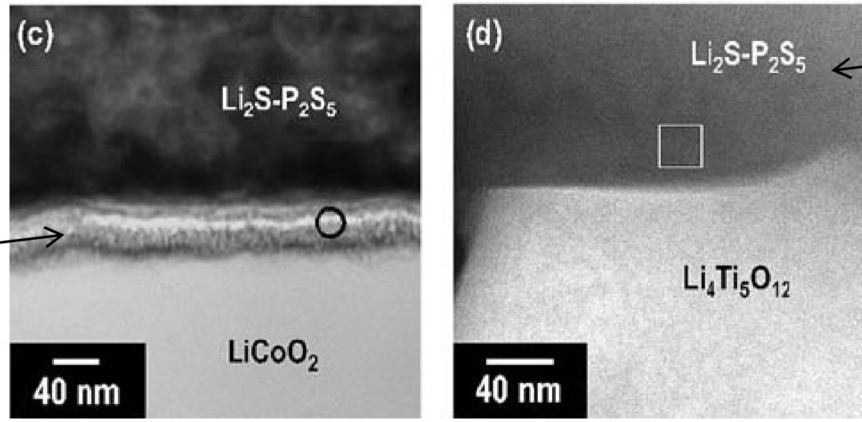

Fig. 7 HAADF-STEM images of the interface between the $LiCoO_2$ or $Li_4Ti_5O_{12}$ active material and the solid electrolyte in the composite electrodes pressed at room temperature ((a) and (b)), and pressed at 210 °C ((c) and (d)).

Tatsumisago and coworkers,
J. Mater. Chem. 21 (2011) 118.

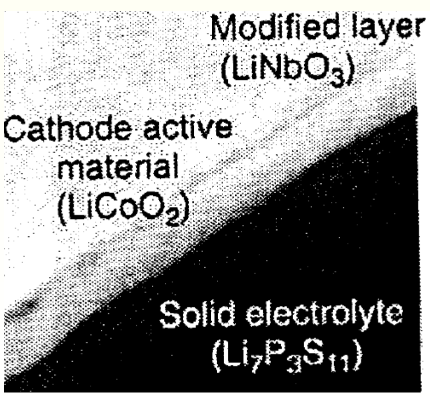

Coating of cathode with protective layer,

e.g. $LiNbO_3$ (thickness in the range of 10 nm)

Solid-State Li-S-Batteries with Li_2S-P_2S_5 Glass as Electrolyte

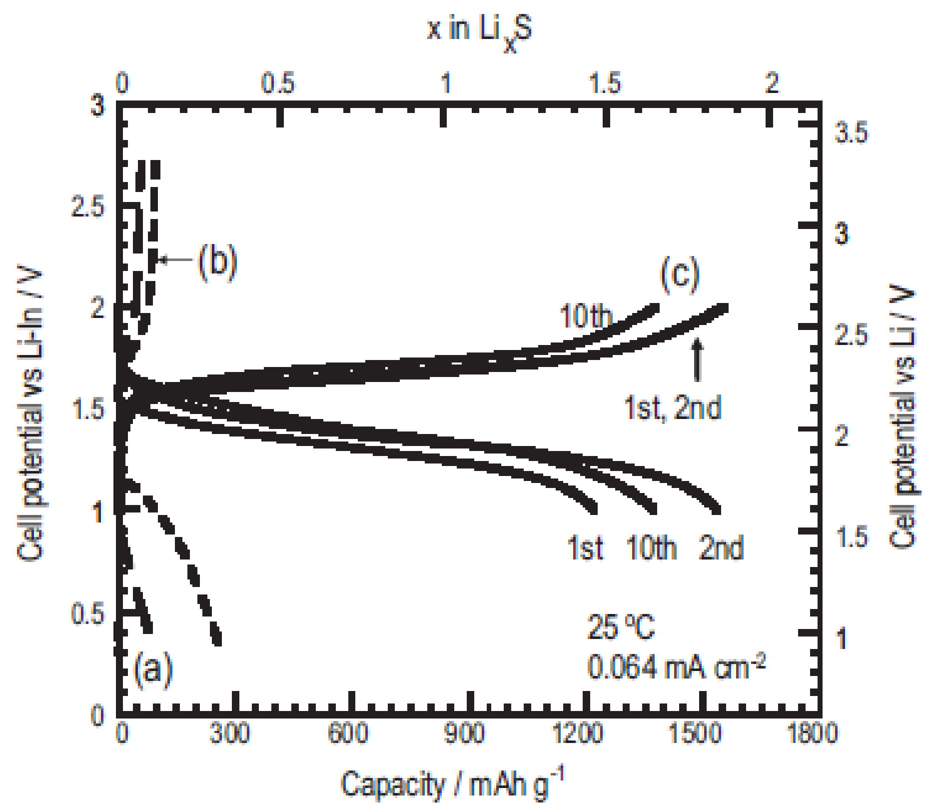

Fig. 3. Charge–discharge curves of all-solid-state cells of Li–In/80Li_2S·20P_2S_5 glass–ceramic/S using (a) (S + AB + SE), (b) (S – AB + SE), and (c) S–AB–SE electrodes as the working electrode.

Tatsumisago and coworkers, Electrochim. Acta 56 (2011) 6055.

At low charge/discharge rates, the battery capacity is close to the theoretical capacity.

Lithium-Air Batteries

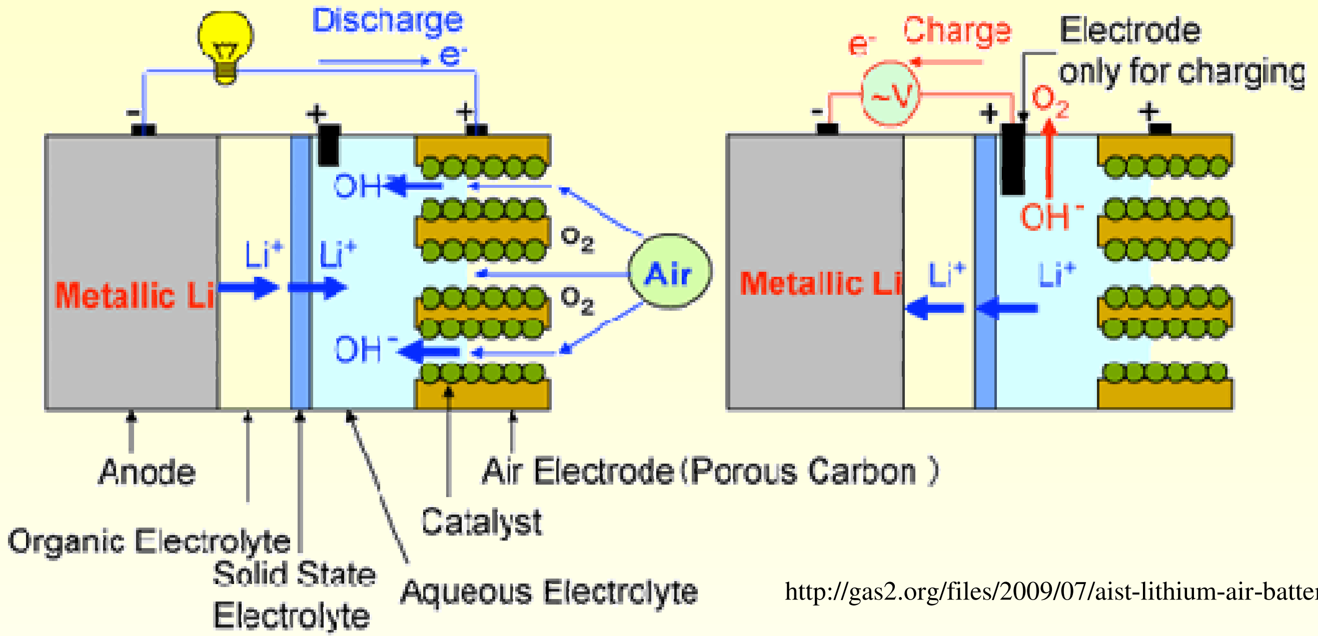

http://gas2.org/files/2009/07/aist-lithium-air-battery.png

$$O_2 + 2\,Li \rightarrow Li_2O_2 \qquad\qquad EMF \approx 3.1\ V$$

$$\text{theoretical energy density} \approx 3{,}6\ \frac{\text{kWh}}{\text{kg } Li_2O_2}$$

(comparable to mechanical energy from 1 kg gasoline)

Crystalline Fast Lithium-Ion Conductors

NASICON

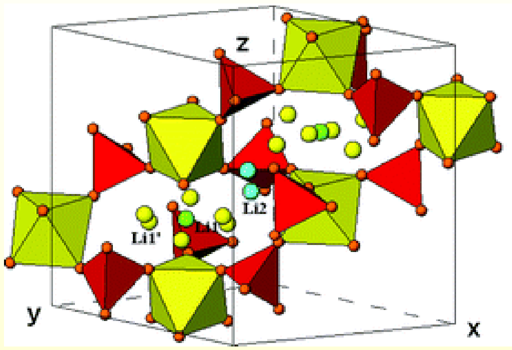

$Li_{1+x}Al_xGe_{2-x}(PO_4)_3$ (LAGP)

$Li_{1+x}Al_xTi_{2-x}(PO_4)_3$ (LATP)

Perovskite

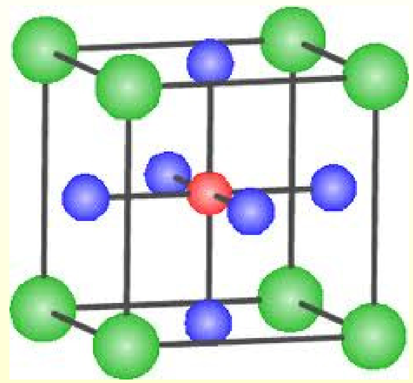

$Li_{3x}La_{2/3-x}TiO_3$

Garnet

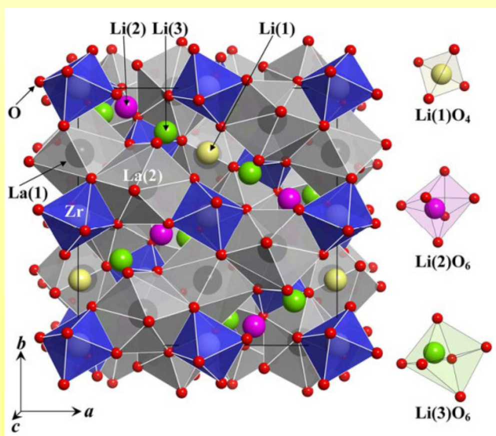

$Li_7La_3Zr_2O_{12}$

Brick Layer Model for Grain Boundary Ion Transport

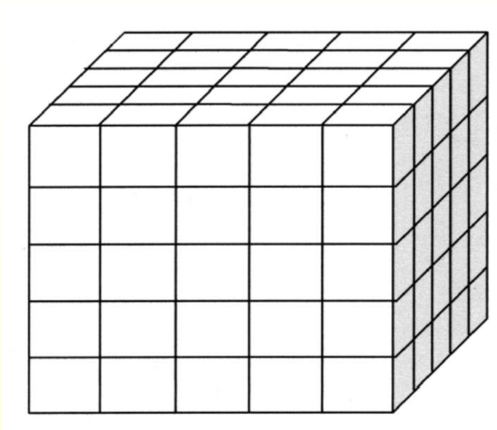

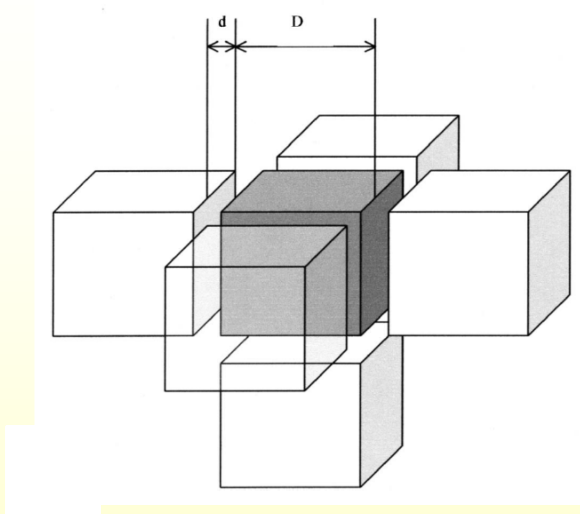

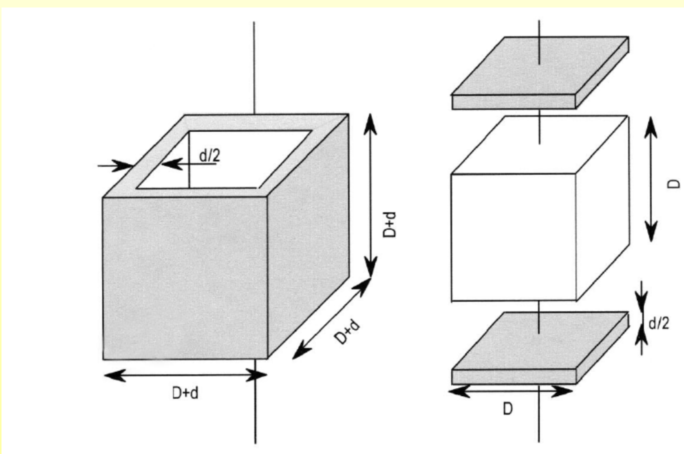

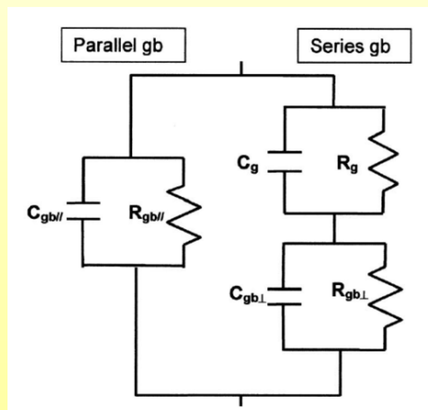

Parallel gb conduction is only then relevant, if

- $\sigma_{gb} >> \sigma_g$ or
- D is comparable to d

Ref: R. Bouchet et al, J. Electrochem Soc 150 (2003) E348; J. Electroceram 16 (2000) 229.

N.J. Kidner, et al., J. Electroceram. 14 (2005) 283; 14 (2005) 293.

Parallel Grain Boundary Conduction in Lithium Ion Conductors

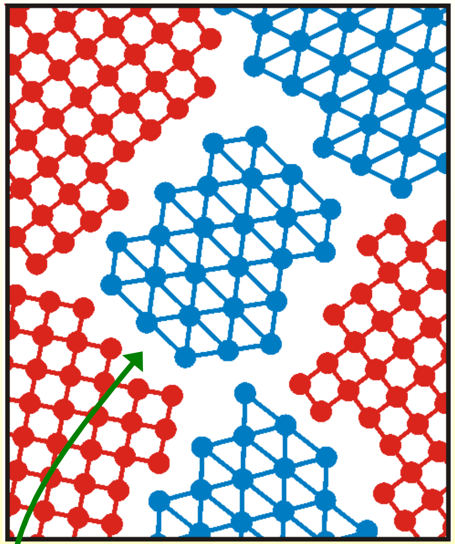

Li_2O - B_2O_3 nanocomposite

Fast Li^+ ion conduction at interfaces

P. Heitjans, S. Indris, *Phys. Cond. Mat.* **15** (2003) R1257.

$LiNbO_3$

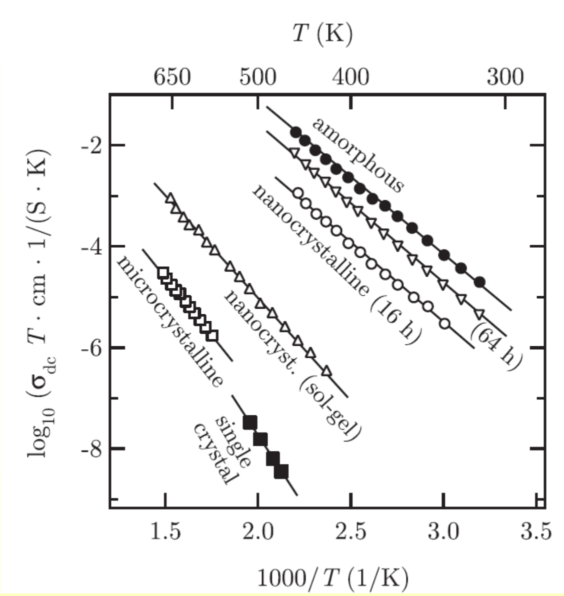

P. Heitjans, M. Masoud, A. Feldhoff, M. Wilkening, *Faraday Discuss.* **134** (2007) 67.

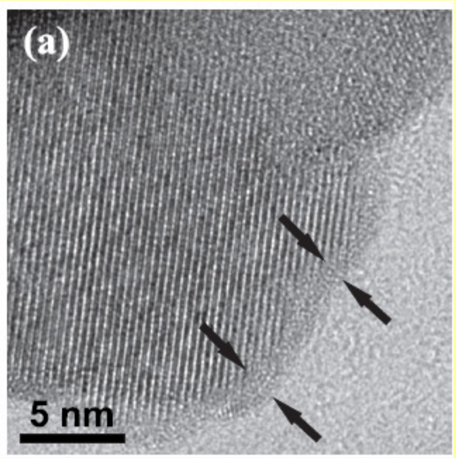

Large amount of *amorphous* $LiNbO_3$ at the boundaries of the nanograins

If parallel grain boundary conduction is negligible:

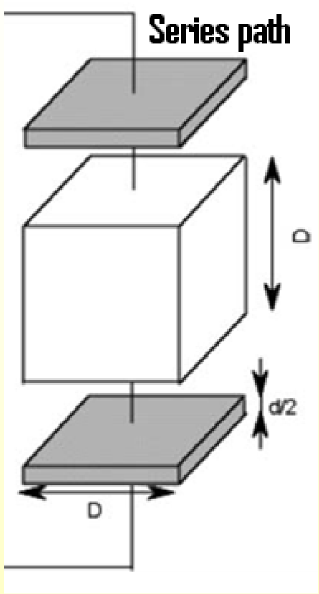

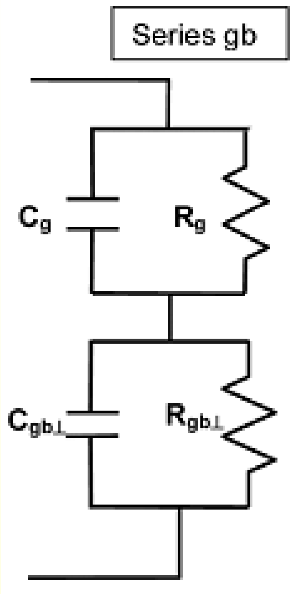

Simple results for ratios of capacitances and resistances:

$$\frac{R_g}{R_{gb\perp}} = \frac{\sigma_{gb}}{\sigma_g} \cdot \frac{D}{d} \qquad \frac{C_g}{C_{gb\perp}} = \frac{\varepsilon_g}{\varepsilon_{gb}} \cdot \frac{d}{D}$$

Nano-Grain Composite Model

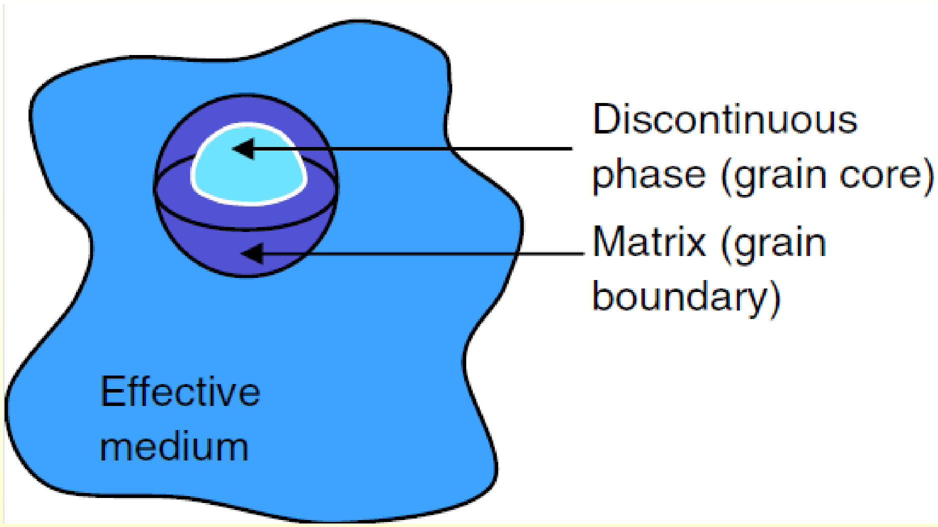

Kidner et al.,
J. Am. Ceram. Soc.
91 (2008) 1733.

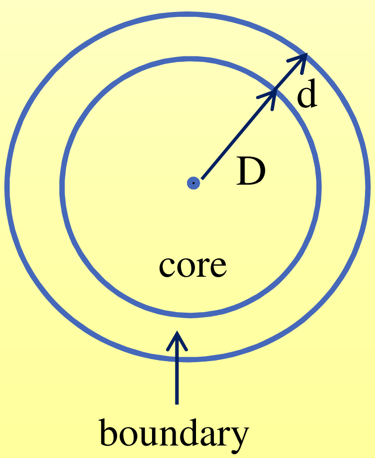

if $D \gg d$

$$\frac{C_{gb}}{C_{gc}} = \frac{\varepsilon_{gb}}{\varepsilon_{gc}} \cdot \frac{D}{d}$$

$$\frac{R_{gb}}{R_{gc}} = \frac{\sigma_{gc}}{\sigma_{gb}} \cdot \frac{d}{D}$$

in agreement with brick layer model

TEM Images of $Li_{1.5}Al_{0.5}Ge_{1.5}(PO_4)_3$ (LAGP)

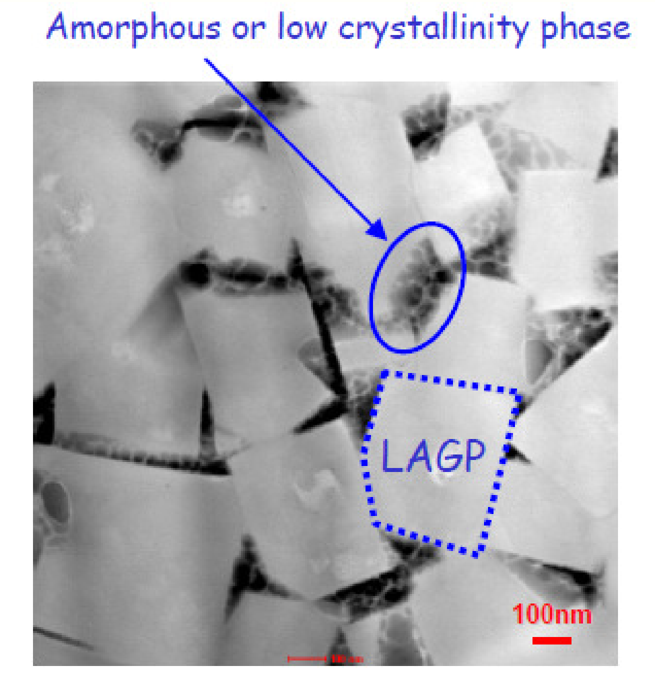

C. R. Mariappan, C. Yada,
F. Rosciano, B. Roling,
J. Power Sources 196 (2011) 6455.

(i) Existence of impurity phases (e.g. $AlPO_4$) and
amorphous phases with low ionic conductivity

(ii) Contact area between grains is lower than assumed in the BLM

Impedance Spectrum of $Li_{1.5}Al_{0.5}Ge_{1.5}(PO_4)_3$ (LAGP)

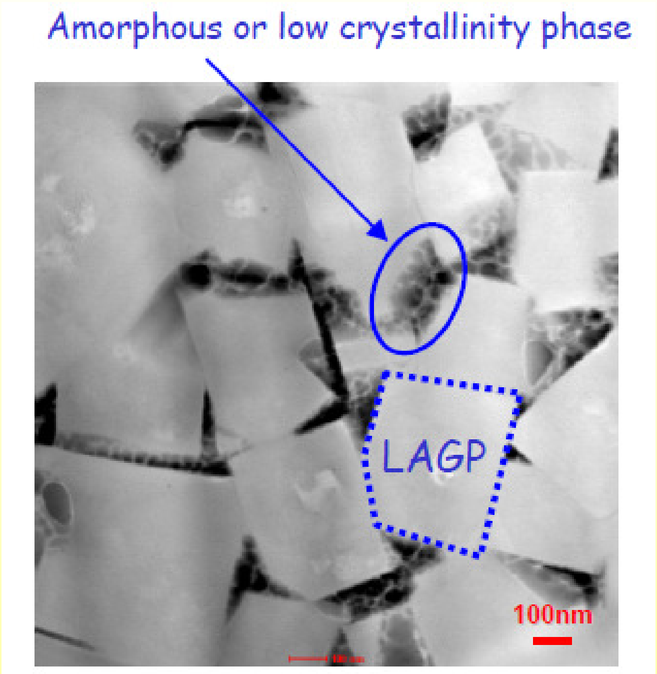

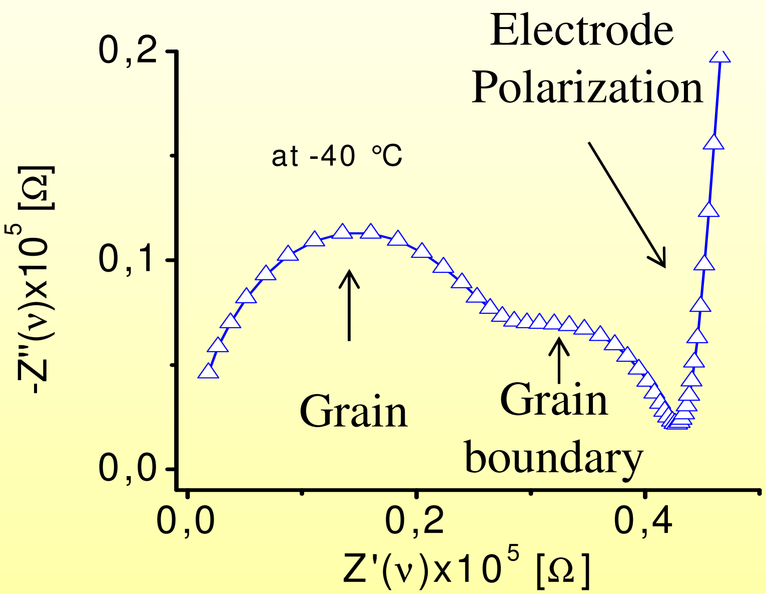

C. R. Mariappan, C. Yada, F. Rosciano, BR, *J. Power Sources* **196** (2011) 6456.

Grain Conductivity and Total Conductivity of LAGP

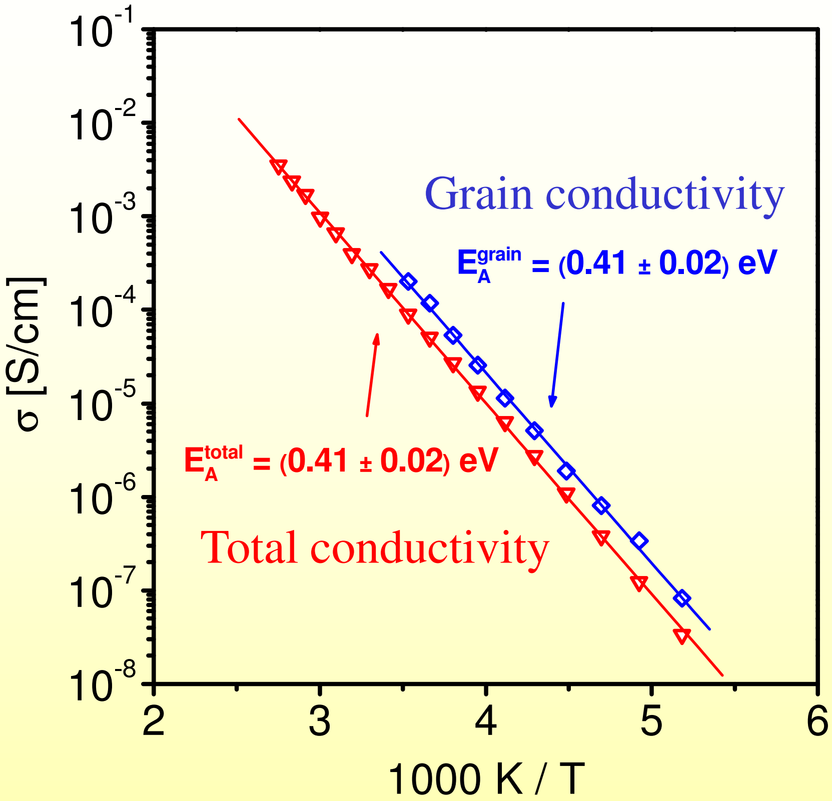

Grain conductivity

$$\sigma_g = \frac{1}{R_g}\left(\frac{d}{A}\right)$$

Total conductivity

$$\sigma_t = \frac{1}{\left(R_g + R_{gb}\right)}\left(\frac{d}{A}\right)$$

Grain and grain boundary resistance are almost identical.

Activation energies are identical.

➡ Purely geometrical current constriction due to limited grain contact area

C. R. Mariappan, C. Yada, F. Rosciano, B. Roling, J. Power Sources 196 (2011) 6455.

Finite-Element Calculations by Fleig and Maier

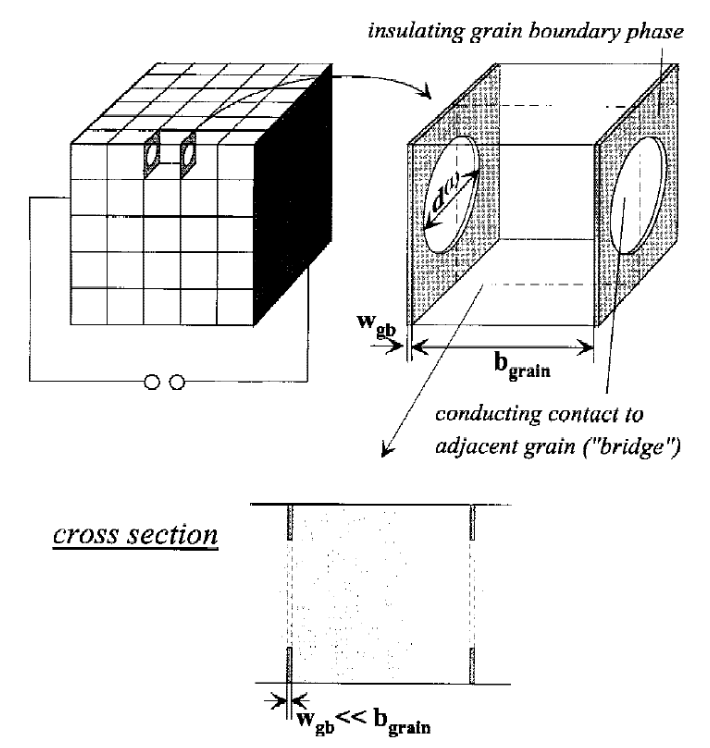

J. Fleig, J. Maier, J. Am. Ceram. Soc 82 (1999) 3485.

$$\frac{R_{gb}}{R_g} \approx \frac{1}{\sqrt{4\,\alpha}}$$

Fraction of contacted area

$$\alpha = A_{contact} \,/\, A_{grain}$$

For LAGP:

$R_{gb} \approx R_g$ ➡ $\alpha \approx 0.25$

in reasonable agreement with TEM results

Impedance Spectroscopy on Ohara Glass Ceramic (commercial)

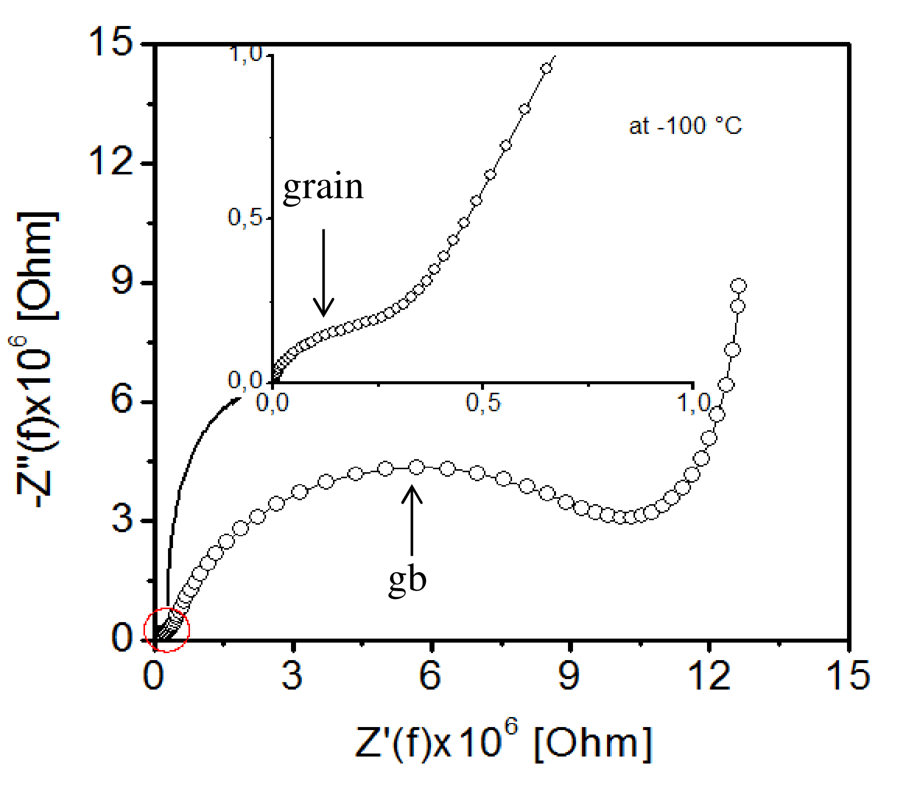

$Li_{1+x}Al_xTi_{2-x}(PO_4)_3$
doped with various
other oxides

Grain boundary resistance
is more than one order of magnitude
higher than grain resistance

Arrhenius Plot of Grain and Grain Boundary Resistance

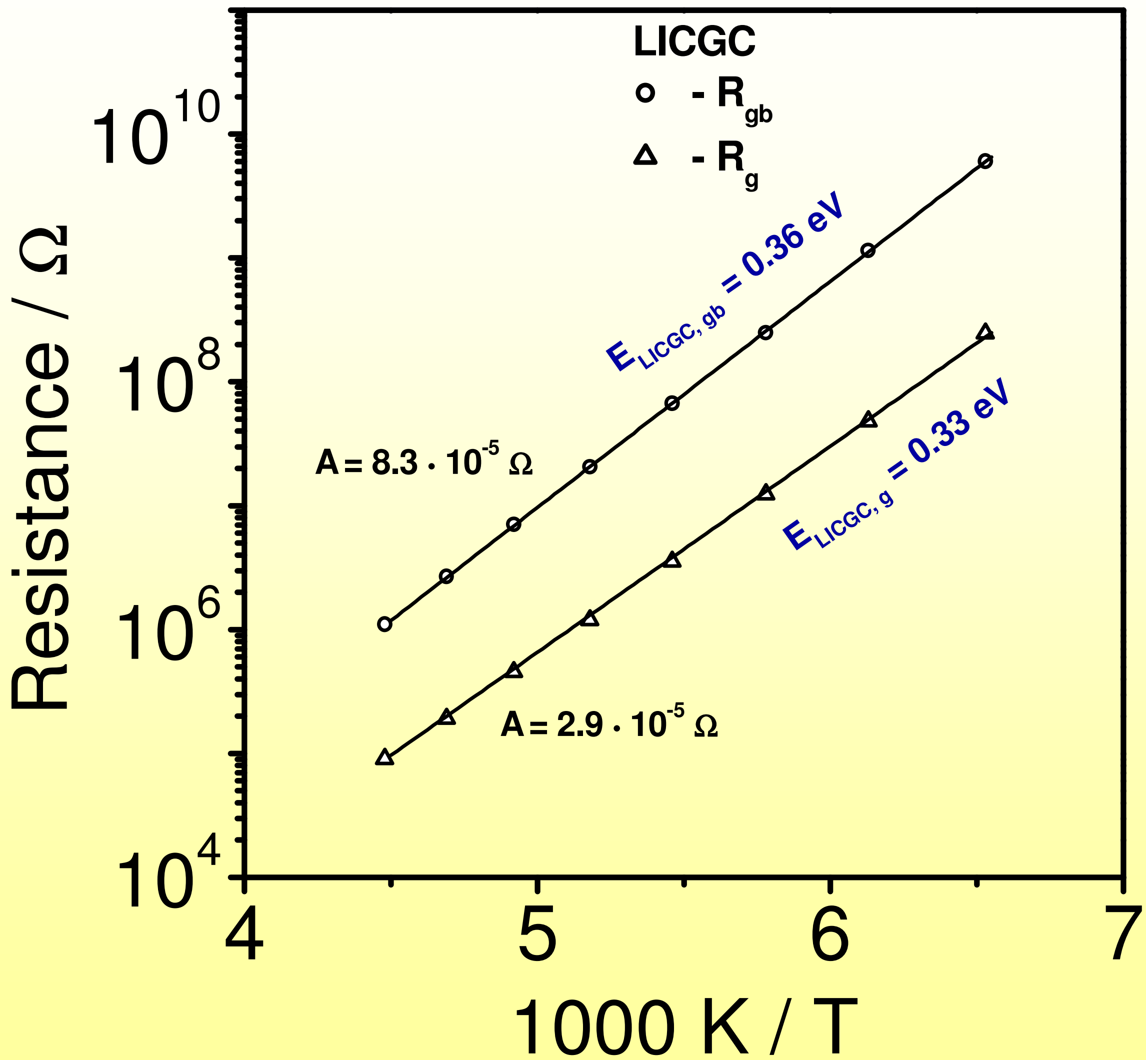

C. R. Mariappan, M. Gellert, F. Rosciano, C. Yada, B. Roling, Electrochem. Comm. **14** (2012) 25.

Ohara Glass Ceramic

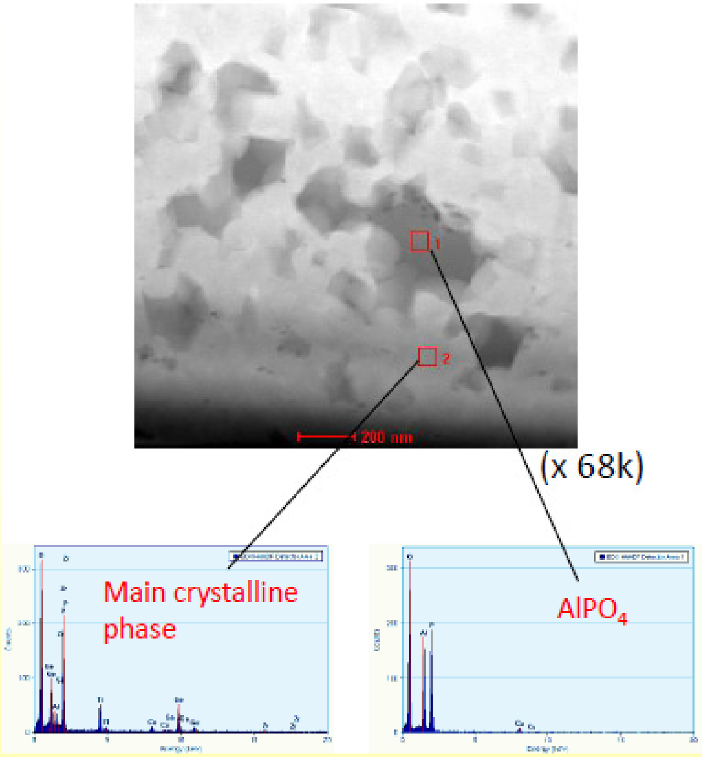

Grain conductivity at room temperature:

$$\sigma_{grain} \approx 10^{-3}\ S/cm$$

$$E_A^{grain} = 0.33\ eV$$

Grain boundary conductivity at room temperature:

$$\sigma_{grain\ boundary} \approx 10^{-4}\ S/cm$$

$$E_A^{grain\ boundary} = 0.36\ eV$$

Origin of higher activation energy of grain boundary conductivity?

Space charge layers? Mechanical stresses?

Space Charge Model

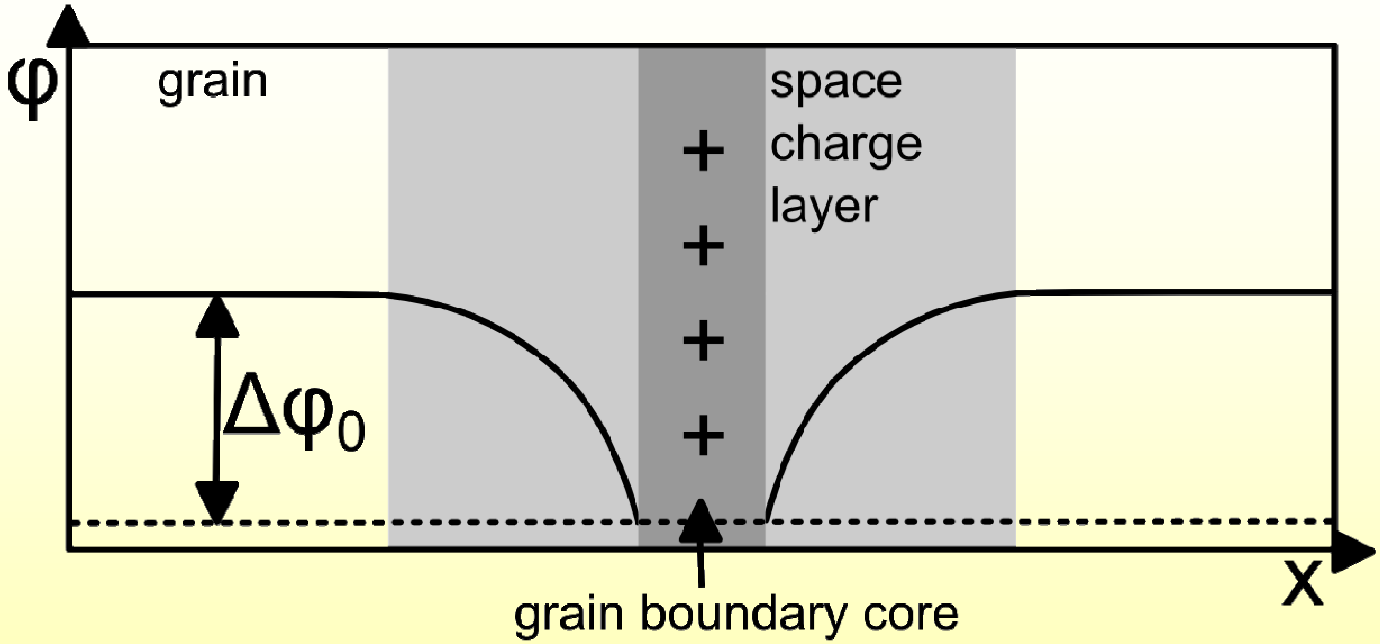

- Charged gb core with oppositely charged space charge layer
- Space charge layer results in electrostatic barrier for ion transport;

  Important: Single barrier

Well established in the field of oxide ion conductors

Measurements with DC Bias on CeO_2 doped with 1% Y_2O_3

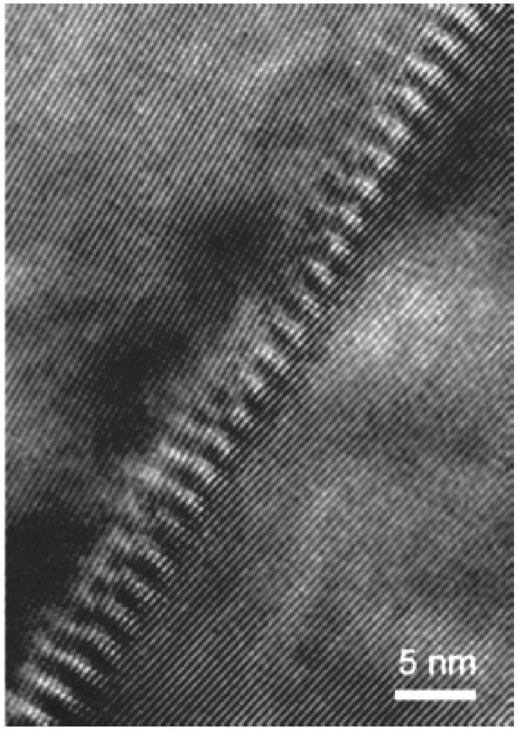

Figure 1. HRTEM of grain boundary in 1.0 mol % Y_2O_3-doped CeO_2. The moiré rings are also visible.

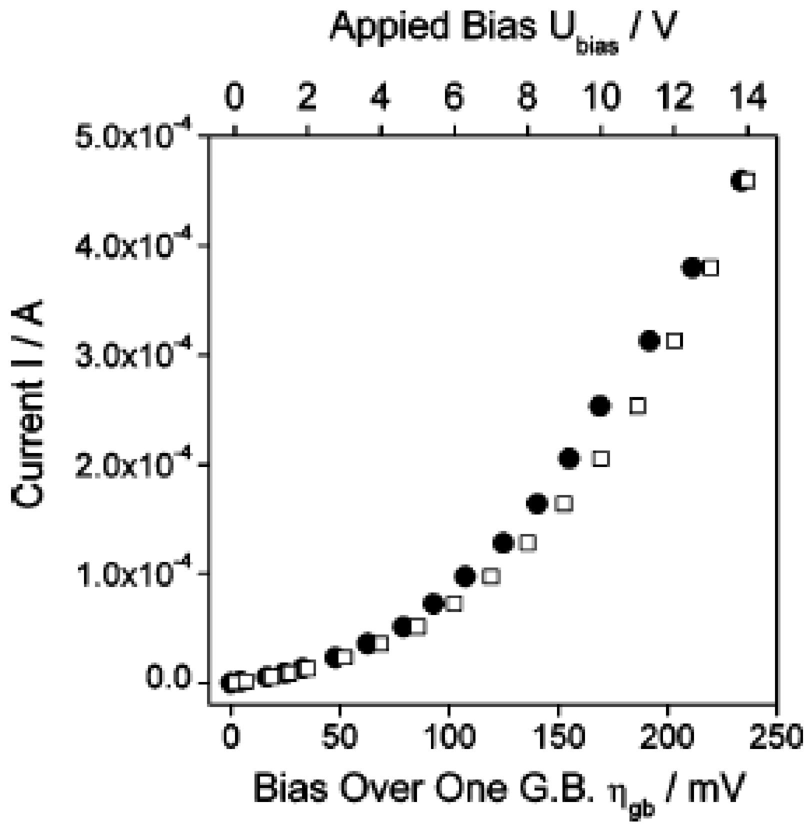

Figure 3. Current I as a function of bias over one grain boundary η_{gb} (filled circles). For comparison the current I-applied bias U_{bias} relation is also plotted (open squares).

Guo, Waser et al.,
Electrochem. Solid State Lett.
8 (2005) J1 and 8 (2005) E67.

Height of
space charge barrier:
about 0.4 eV

High-Voltage Measurement System

Novocontrol Alpha-AK High Performance Frequency Analyser, equipped with:

- High-Voltage Amplifier Trek model 623B
- Novocontrol HVB4000 High-Voltage Impedance Interface

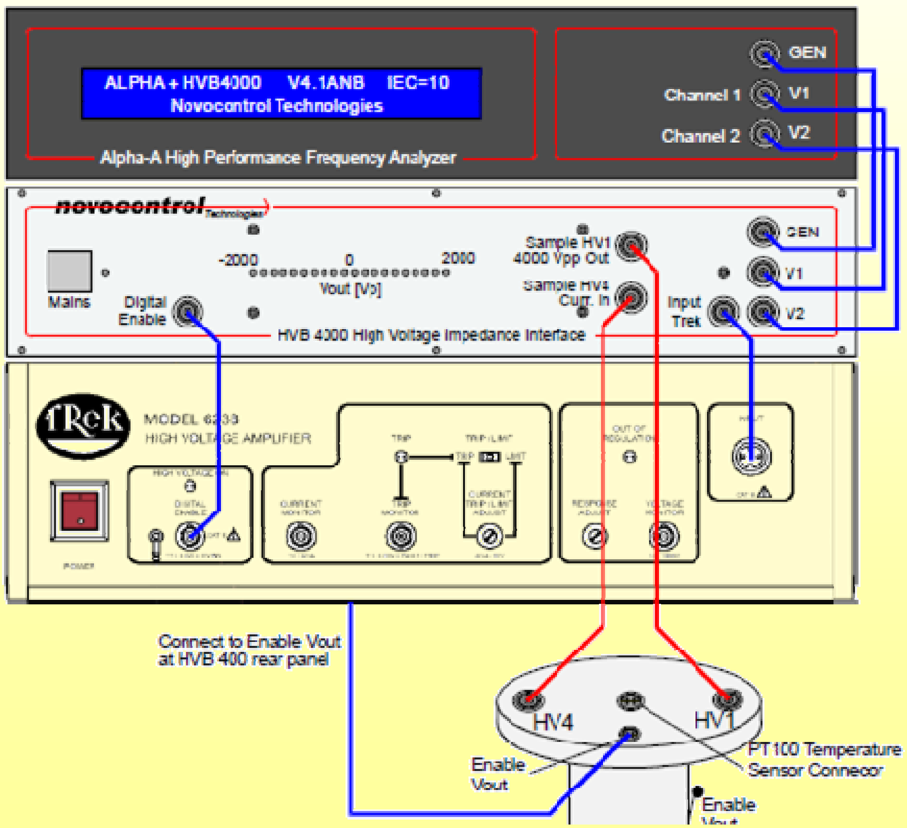

- Frequency range: 3 μHz - 10 kHz
- Maximum amplitude of ac voltage: 2 kV
- Current resolution: 5 fA

Nonlinear Impedance Spectroscopy with High AC Voltages

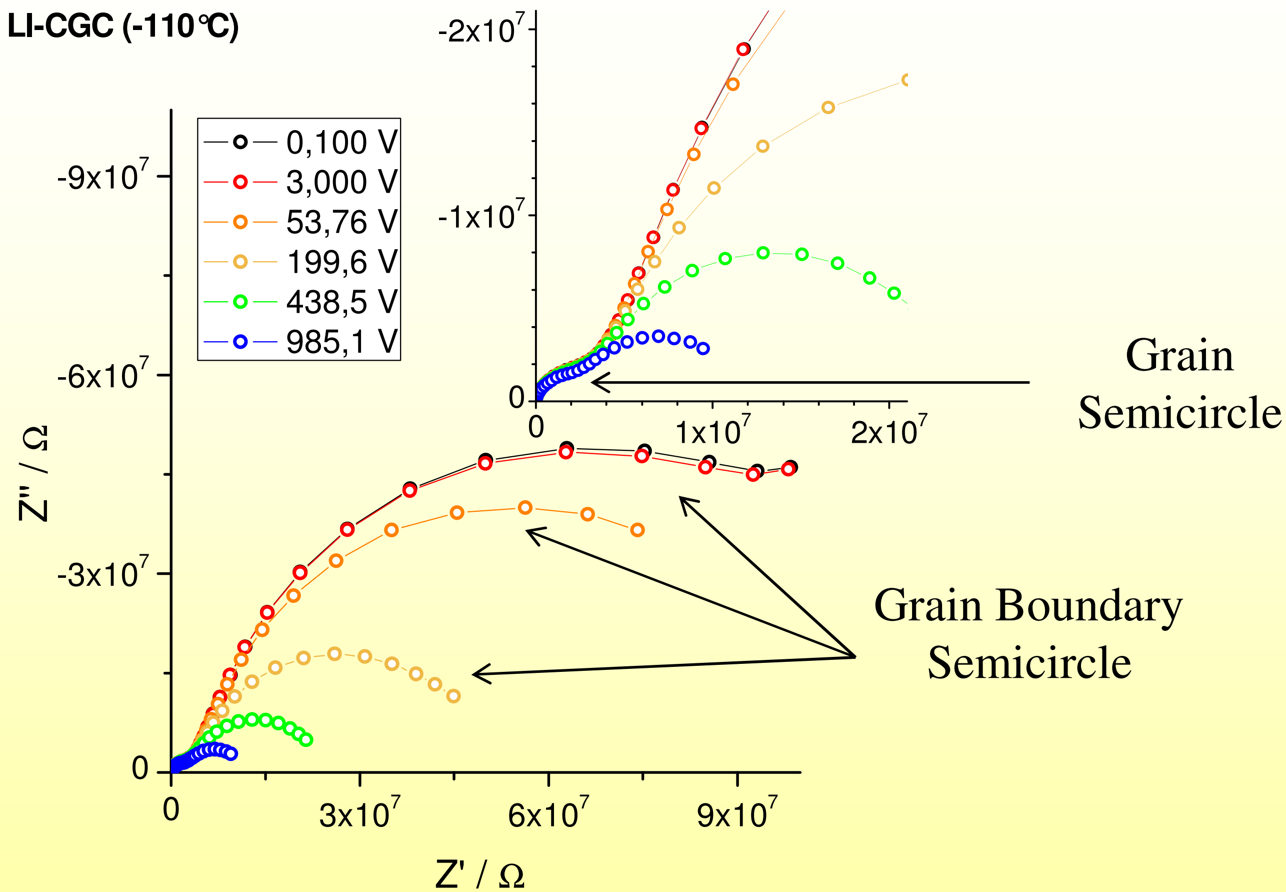

- **Almost 1 V ac voltage per single grain boundary can be applied without any irreversible changes of the grain boundary properties**
- **Grain boundary resistance decreases with increasing voltage**

Grain Boundary Conductivity vs. AC Voltage per Single Grain Boundary

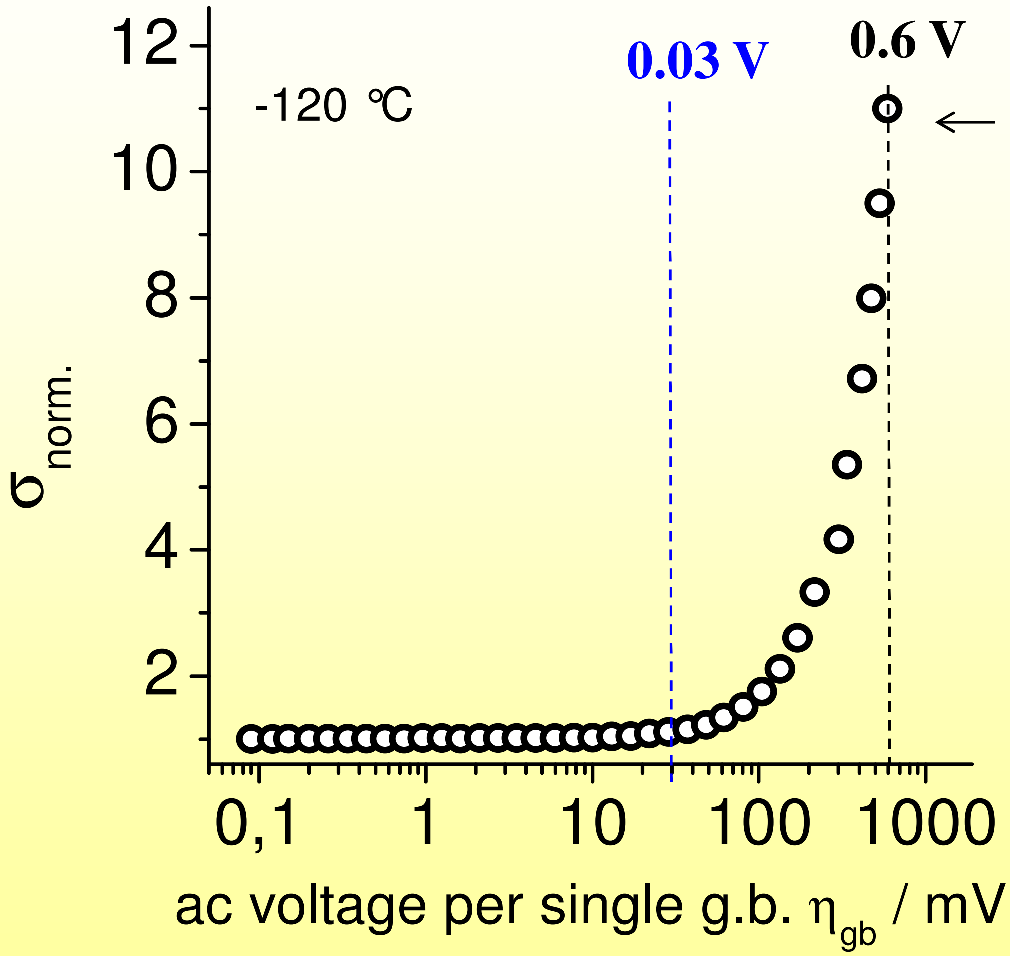

Grain boundary resistance is still slightly higher than grain resistance

If a **single higher barrier** existed at each grain boundary

An external voltage of about 30 mV should sufficient for decreasing the grain boundary resistance to the level of the grain resistance

Influence of High Voltages on Ion Transport Across Grain Boundary

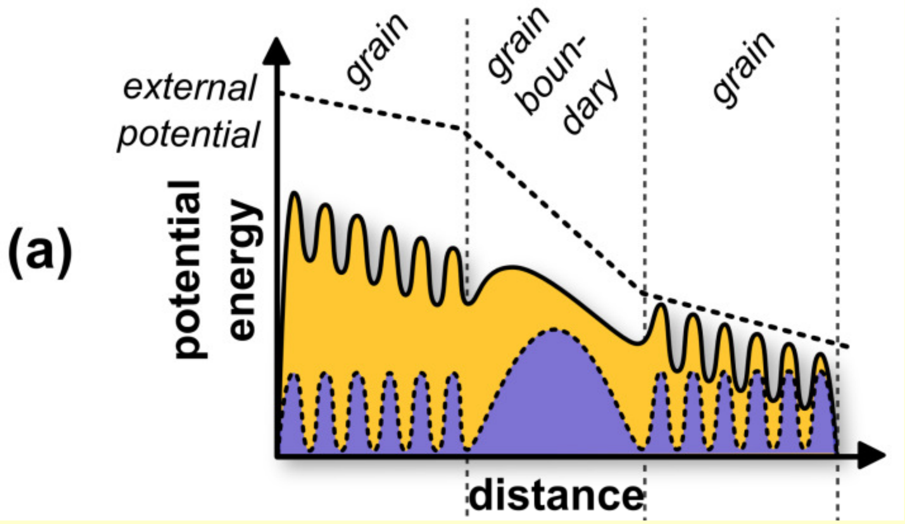

Influence of High Voltages on Ion Transport Across Grain Boundary

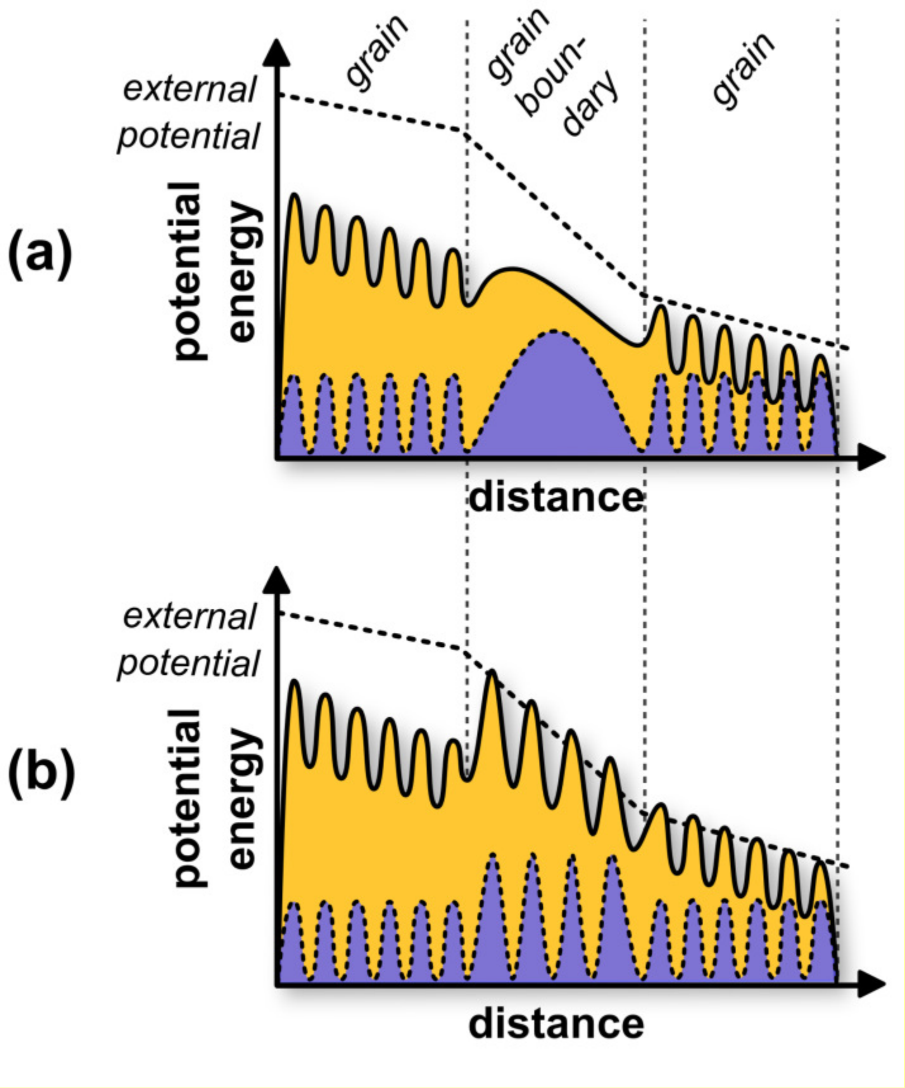

Estimation of Grain Boundary Thickness

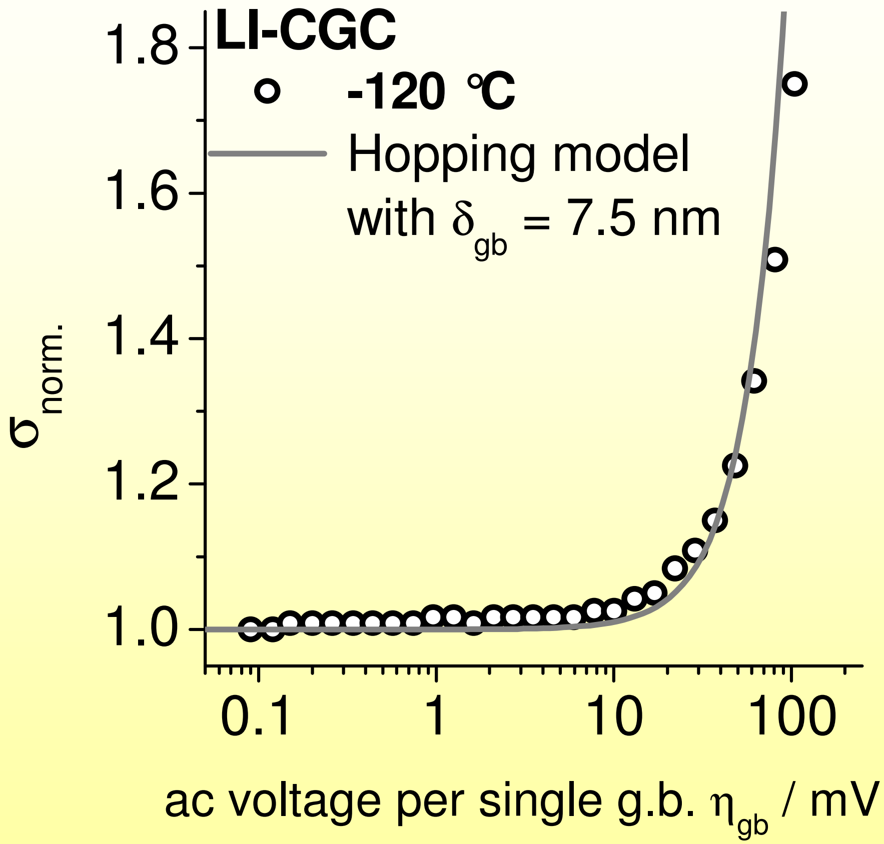

Assumption:

Field dependence of gb conductivity follows universal behaviour of thin ion-conducting layers.

Thickness of grain boundary: about 7.5 nm

HR-TEM Images of Grain Boundaries

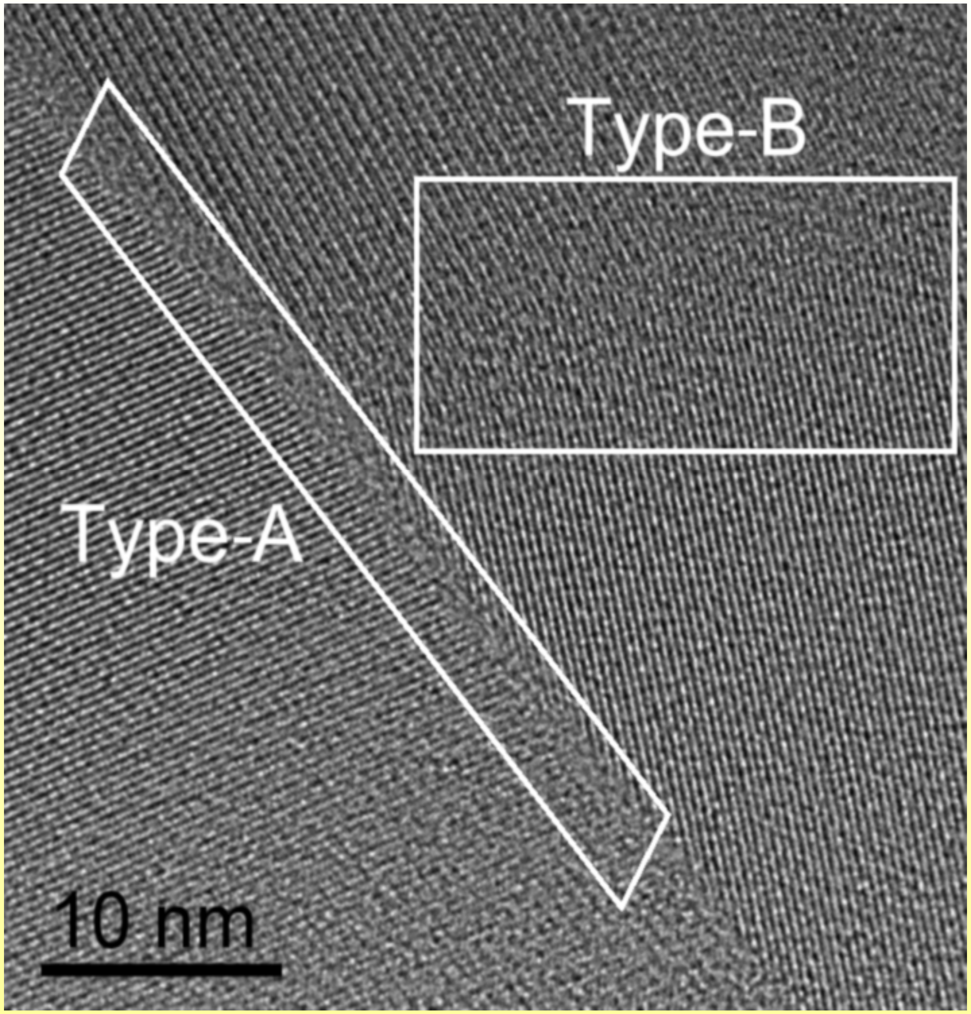

Type-B Grain Boundary:

- Layer between grains with similar lattice orientation:
- High degree of crystallinity
- Mechanical stresses may lead to slighly higher activation energy
- Thickness: about 5-10 nm

Type-A Grain Boundary:

Amorphous layer between grains with strongly dissimilar lattice orientation

→ Highly resistive

Model for Grain Boundary Transport

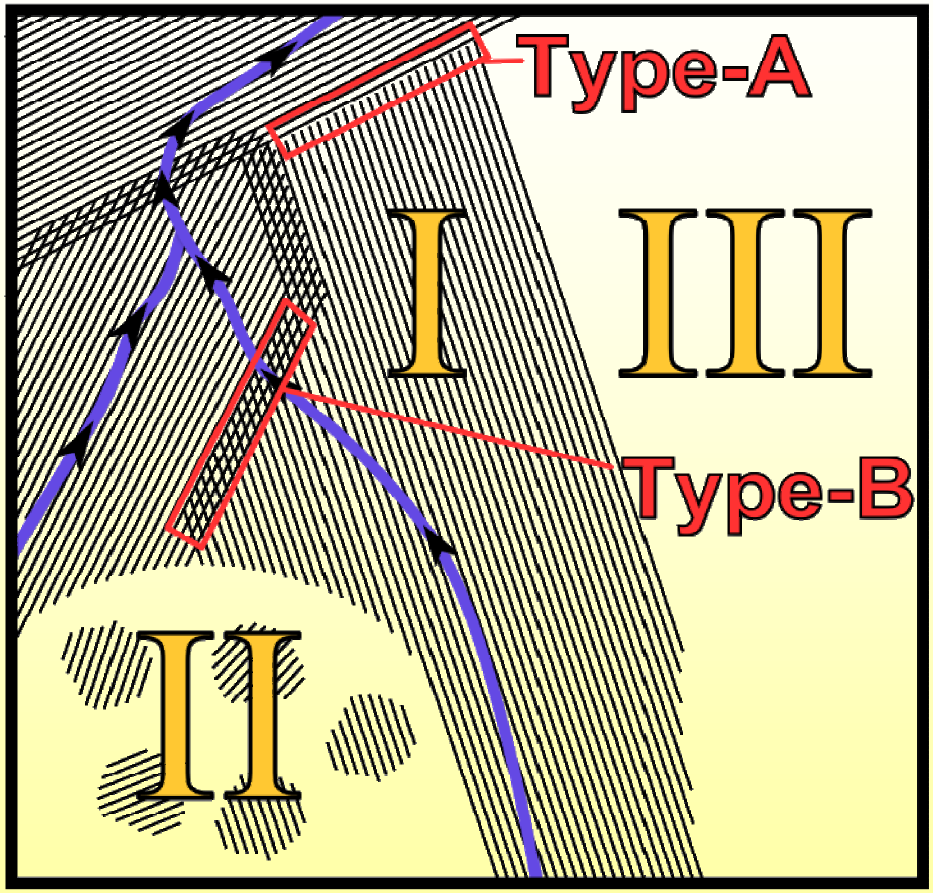

Blue lines: Ion transport pathways

Conclusions

$Li_{1.5}Al_{0.5}Ge_{1.5}(PO_4)_3$ (LAGP)

- Grain and grain boundary resistance exhibit the same activation energy.
  → **Purely geometrical current constriction**; **fraction of contacted area: about 25%**

Ohara Glass Ceramic ($Li_{1+x}Al_xTi_{2-x}(PO_4)_3$ doped with other oxides)

- Grain boundary resistance exhibits a slightly higher activation energy than the grain resistance.
- Nonlinear impedance spectra provide strong indication that the grain boundary resistance is **not** caused by **a single (space charge) barrier**, but by **several serial barriers**
- Fit of nonlinear impedance data suggests that the **thickness of the grain boundaries is in the range 5-10 nm.**
- HR-TEM images reveal type-A (amorphous) and **type-B** (high degree of crystallinity) **grain boundaries**.
- **Thickness of type-B** grain boundaries is, in fact, in the range 5-10 nm. **Mechanical stresses** may lead to slightly higher activation energy.

Many thanks

for

your attention!